

# Introduction of Curvature in Amphipathic Oligothiophenes for Defined Aggregate Formation

Patrick van Rijn,<sup>[a]</sup> Dainius Janeliunas,<sup>[a]</sup> Aurélie M. A. Brizard,<sup>[a]</sup> Marc C. A. Stuart,<sup>[b]</sup> Rienk Eelkema,<sup>[a]</sup> and Jan H. van Esch<sup>\*[a]</sup>

**Abstract:** In this study the possibility to control the size and shape of self-assembled structures through the local curvature of their molecular building blocks has been investigated. To this end a series of amphipathic conjugated oligothiophenes with a well-defined curvature of their backbone has been designed and synthesized. The molecular (local) curvature of these oligothiophenes resulted from a preference for *cis* instead of *trans* conformations at specific positions along the oligothiophene backbone, which can be controlled by the sequence of hydrophilic

and hydrophobic groups, while their ratio was kept constant. The self-assembly of ter-, sexi-, and dodecathiophenes appeared to be a low-cooperative process, involving the formation of pre-micellar aggregates at sub-millimolar concentrations, which at concentrations in the millimolar regime transformed into micelles and cylindrical micelles. The aggregates display fine

**Keywords:** amphiphiles • oligothiophenes • photophysics • self-assembly • sulfur

structures with dimensions reminiscent of the thiophene molecules. The structure–morphology relationship of the ter- and sexithiophenes could be described by conventional packing theory. However, with the dodecathiophene, the backbone curvature governed the formation of cylindrical aggregates with a well-defined diameter. These results demonstrate that it is possible to control the aggregation morphology of simple amphipathic oligothiophenes by implementation of an additional structural motif namely, the curvature.

## Introduction

Over the past decades the self-assembly of molecular components has become a major approach for the construction of nanostructured materials and architectures with potential applications in, for example, biomedical materials, drug delivery, and molecular devices.<sup>[1]</sup> However, the polydispersity in size of many self-assembling systems<sup>[2]</sup> puts serious limitations on the use of self-assembly approaches for hierarchical


structure formation<sup>[3]</sup> and hampers the application of self-assembled aggregates in, for instance, optical, electronic, and magnetic devices.<sup>[4]</sup>

Several strategies have been developed to obtain aggregates by self-assembly of molecular components that are well defined in size and/or shape. For instance the use of small, convergent molecular components that self-assemble through multiple cooperative, specific and directional interactions,<sup>[5]</sup> has been particularly successful to obtain a variety of nano-objects composed of a well defined number of molecular components, like capsules,<sup>[6]</sup> grids,<sup>[7]</sup> helices,<sup>[8]</sup> and so forth.<sup>[9]</sup> So far, these discrete assemblies have not found many applications, because the tight correlation between molecular and supramolecular structure hampers the ability to introduce functionality.

Another generic strategy to create well-defined supramolecular assemblies is to make use of a repulsive interaction that increases with growing aggregate size, thereby creating a minimum at the free-energy surface for a specific aggregate size. There are several factors that influence the free-energy surface, for example, head group repulsions with some surfactants leading to spherical or rodlike micelles<sup>[1,10]</sup> and to other more exotic structures,<sup>[11]</sup> the chiral twist which

[a] Dr. P. van Rijn, D. Janeliunas, Dr. A. M. A. Brizard, Dr. R. Eelkema, Prof. Dr. J. H. van Esch  
Self assembling systems, Faculty of Applied Sciences  
Delft University of Technology, Julianalaan 136  
2628 BL, Delft (The Netherlands)  
Fax: (+31) 152784289  
E-mail: j.h.vanesch@tudelft.nl

[b] Dr. M. C. A. Stuart  
Electron microscopy  
Groningen Biomolecular Sciences and Biotechnology Institute  
University of Groningen, Nijenborgh 4  
9747 AG, Groningen (The Netherlands)

 Supporting information for this article is available on the WWW under <http://dx.doi.org/10.1002/chem.201001831>.

limits the width of the surfactant ribbons,<sup>[12]</sup> and steric repulsion in peptide ribbons<sup>[13]</sup> and block-copolymers<sup>[14]</sup> leading to ordered mesophases and finite assemblies like Stupp's mushrooms.<sup>[15]</sup> All these molecular self-assembly properties can be considered as manifestations of this repulsion, and have been described in (semi-)quantitative models by, for example, Bates and Israelachvili.<sup>[14,16]</sup> These models have in common that they all stress the relationship between the curvature and object dimension. However, the relationship between surfactants, peptides, and block copolymers and the local curvature of the self-assembled objects formed by them is very diffuse and hampers rational control and design.

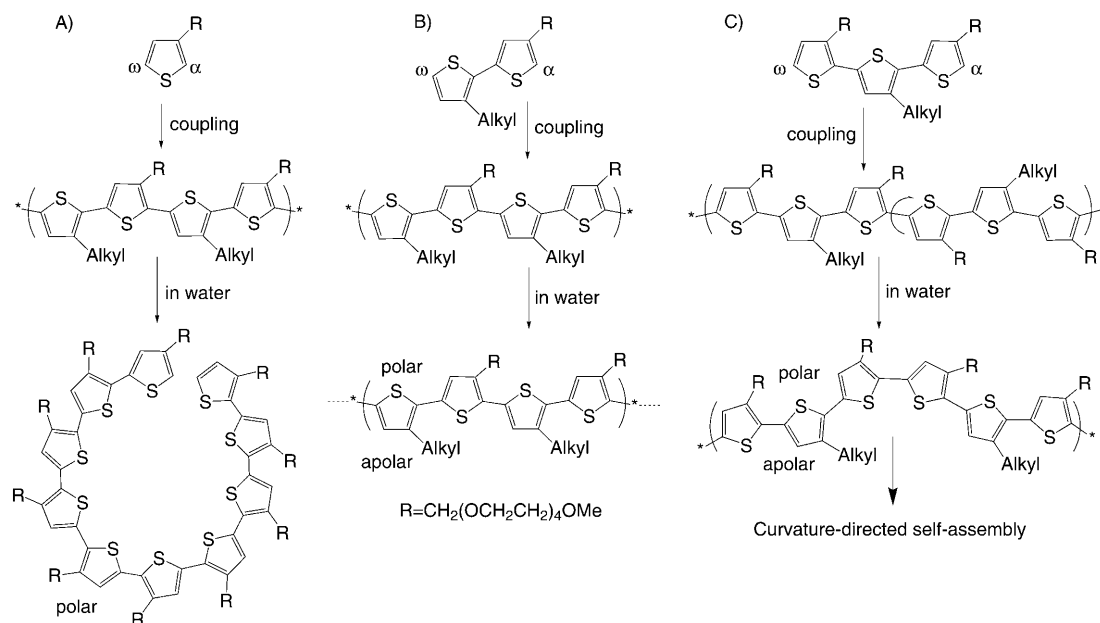
Clearly, the development of functional nanodevices and synthesis of mesoscopic materials using self-assembly methods would greatly benefit from novel approaches to generate nano-objects. The challenge is to develop new molecular components with a precise and tuneable control of their curvature that upon self-assembly will lead to nanostructures with well-defined shape and size, and allow the controlled spatial positioning of functional moieties. This would be also of particular interest in combination with opto-electronically active species. Over the past decade there has been a strongly growing interest in molecular and supramolecular electronics with nanoscale structural features, obtained by the self-assembly of molecular components.<sup>[17,18]</sup> Self-assembled electronic structures like micelles, fibres, tubes, bilayers, and vesicles have been prepared from a wide variety of electronically active molecular building blocks in organic solvents<sup>[19–24]</sup> and to a limited extent also in water.<sup>[25–27]</sup> Alternatively, hydrophobic opto-electronic molecules have been

used in combination with surfactant assemblies, for example, as sensors for biological species like proteins and DNA or as a visualisation tool for membranes.<sup>[28–31]</sup> Clearly, conjugated self-assembled systems in water are of great interest because of their potential biocompatibility.

Here we report on amphipathic oligothiophenes that self-assemble into cylindrical aggregates of discrete diameter in water as a consequence of the well-defined curvature of the oligothiophene backbone. The curvature of the oligothiophene backbone arises from a preference for a *cis* instead of *trans* conformation at specific positions due to reorientation of the polar and apolar side-chains in aqueous environment. First, we describe the design and synthesis of the amphipathic oligothiophenes, and then we continue with an investigation of their self-assembly behavior in water. We conclude this paper with a preliminary study of the photophysical properties of the oligothiophenes and their assemblies. Our results demonstrate that it is possible to control the aggregation morphology of simple amphipathic oligothiophenes by implementation of an additional structural motif namely, the curvature.

## Results and Discussion

**Design of curved amphipathic oligothiophenes:** To obtain an amphipathic structure with well-defined curvature we built upon amphiphilic terthiophenes, which can easily be extended to longer oligothiophenes by standard cross-coupling methodologies (Scheme 1C, top structure). In Scheme 1, the effect of the sequence of hydrophilic and hy-



Scheme 1. Different designs of conjugated oligothiophenes that are formed by coupling of a monomer, leading to an oligomer. When brought into an aqueous environment, they tend to organize themselves: A) non-amphiphilic, hydrophilic, substituted thiophene that folds into a helical structure with the curvature obtained from the *trans* to *cis* reorientation of the thiophene; B) an amphiphilic bithiophene that creates a linear oligomer upon oligomerization and can be used to form Langmuir–Blodgett multi-layers at the polar–apolar interface; C) a terthiophene that is amphiphilic in nature and upon oligomerization the two substituents of the thiophenes that are connected are of similar polarity. This similar polarity makes it possible that a curvature is obtained only with the ability to further self-assemble due to the formed amphipathic character.

drophobic thiophene residues on the folding and self-assembly of longer oligomers is depicted. The simplest structure consists of a linear sequence of hydrophilically substituted thiophenes. It has been found that such structures adopt an all-*cis* conformation between thiophene units, and nicely fold into single helices of well-defined size, which are not amphiphilic and do not aggregate any further after folding.<sup>[32]</sup>

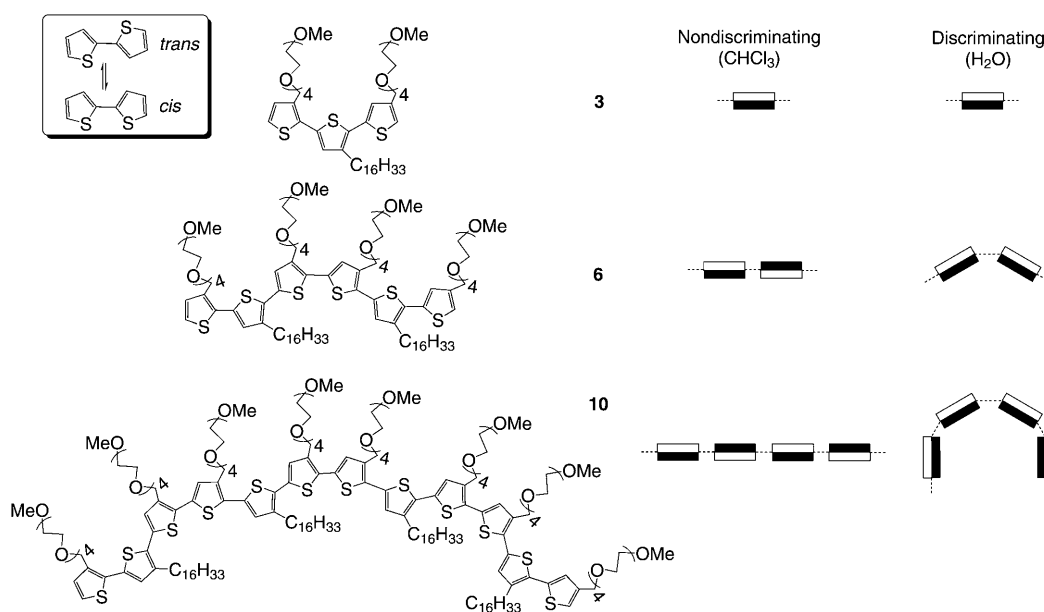
Evidently, the dimensions of the helix are determined by the angle between the *cis*-oriented thiophenes. When an amphiphilic bithiophene is taken as the monomeric structure, it can also be extended to longer structures. For an alternating sequence of hydrophilic and hydrophobic thiophene residues, the oligothiophenes are expected to adopt an all-*trans* conformation, and as a result they are linear and amphipathic in nature. It was found that such thiophenes prefer to self-assemble at the air-water interface and can be used to construct Langmuir–Blodgett multilayers.<sup>[33]</sup> From these simple models it can be seen that the introduction of two neighboring hydrophilic or hydrophobic thiophenes, in an otherwise alternating sequence, would introduce a *cis* conformation in polar environments, which would result in a nonlinear or curved shape of the oligothiophene. Such oligothiophenes with a defined number of hydrophilic–hydrophilic (or hydrophobic–hydrophobic) thiophene neighbors can most conveniently be constructed for terthiophene building blocks, as depicted in Scheme 1 C. It is anticipated that such amphipathic oligothiophenes will be able to self-assemble in a similar fashion as surfactants. However, it is expected that the overall shape or curvature of the oligothiophene will determine the aggregate morphology, rather than the ratio between head group area and hydrophobic tail volume.

It should be noted that regio-regular substituted terthiophenes like the one depicted in Scheme 1 C were preferred as the basic building blocks for longer oligomers, because the different reactivity of the  $\alpha$ - and  $\omega$ -positions allows the synthesis of well-defined isomers. By this approach, unfavorable and unwanted steric interactions, which would disturb the desired *cis* and *trans* conformations, are avoided. The terthiophene itself does not possess any curvature like the longer oligomers as can be seen in Scheme 2. Only coupled terthiophenes will contain *cis* conformations, which will result in curved amphipathic molecules. Evidently, this conformational preference is driven by the different solvent affinity of the alkyl chains and ethylene glycols chain for polar and apolar solvents (Scheme 2).

Based on these assumptions it is now possible to estimate the diameter directly from the molecular structure of the oligothiophenes, and from this, one can predict at least one characteristic length of the resulting supramolecular assemblies. The radii of curvature were calculated for a completely flat conformation of the oligothiophenes, with a *cis* conformation between two identically substituted thiophenes (dihedral angle of 0°), and a *trans* conformation between non-identical substituted thiophenes (dihedral angle of 180°). From basic trigonometry one can determine the basic curvature parameters like curvature radius and cone angle from the dimensions of a partial circular shape (Figure 1).

From the modeling, the dimensions of the chord length ( $a$ ) and height of the arc portion ( $h$ ) can be obtained. The radius of curvature  $R$ , which is equal to  $D/2$  ( $D$  is the diameter), then follows directly from Equation (1).

$$2R = D = \frac{(h^2 + (\frac{a}{2})^2)}{h} \quad (1)$$



Scheme 2. Molecular structures of the three different oligothiophenes (**3**, **6**, and **10**). On the right a schematic representation of the curvature they obtain upon changes in environment, going from a nondiscriminating to a discriminating solvent.

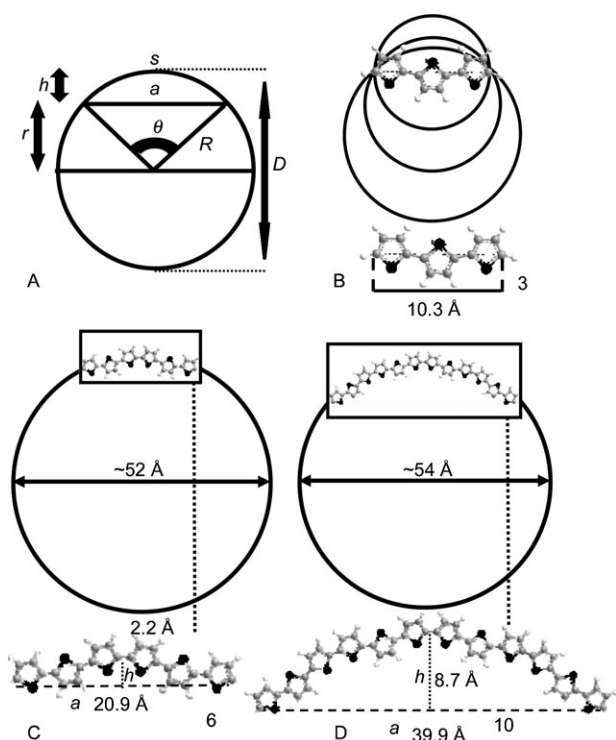


Figure 1. A) A geometrical approach to determine the diameter of the intrinsic curvature of the molecular structure. Here  $R$  is the radius,  $s$  the arc length,  $a$  is the chord length,  $h$  is the height of the arced portion,  $r$  is the height of the triangular portion, and  $\theta$  is the angle between the arc length and the centre of the circle. The modeled curvatures that each oligomer adopts when placed in a discriminating environment (aqueous). B) Compound **3** has an infinite number of potential curvatures which are not expressed. C) **6** and D) **10** do possess a single curvature.

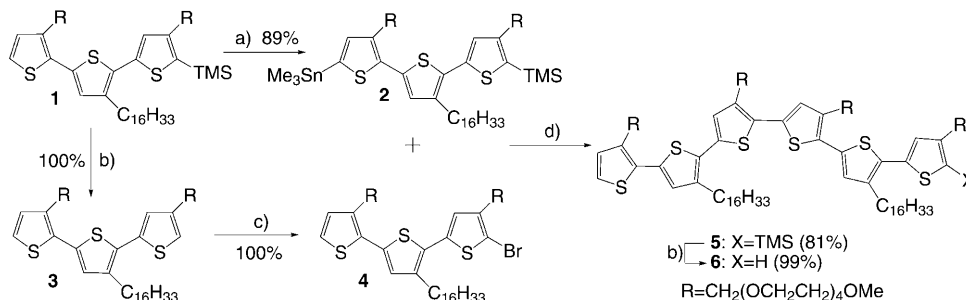
The diameter  $D$  was found to amount to 5.2 and 5.3 nm with cone angles of 26 and 53° for the sexi- (**6**) and dodecathiophene (**10**), respectively. From these values it can be predicted that **6** and **10** are likely to form assemblies with at least one characteristic diameter of approximately 5 nm, with regard to the thiophene moieties, and not accounting for the oligoethylene glycol chains. For terthiophene **3**, the diameter remains undefined because the arc height portion  $h$  is approximately zero. Most likely, the morphology of assemblies of **3** is governed by parameters formulated in the structure-shape concept. Similar values have been obtained by application of other methods, for example, fitting of the oligothiophene coordinates to a circular segment (Figure 1).

**Synthesis of oligothiophenes ter-, sexi, and dodecathiophenes:** The amphipathic oligothiophenes proposed above,

are based on the amphiphilic terthiophene (**3**). The terthiophene **3** is alternately regio-regular substituted with a tetraethylene glycol monomethyl ether and a  $C_{16}$ -alkyl chain, and was synthesized by the sequential addition of hydrophilic- and hydrophobic-substituted thiophenes by using Stille couplings. The terthiophene was then extended by cross-coupling reactions to obtain an amphipathic sexiathiophene (**6**) and a dodecathiophene (**10**). The coupling was performed stepwise in order to maintain the regio-regular structural features to minimize any possible steric interactions of the side-groups, which could influence the implementation of the curvature upon orientation.

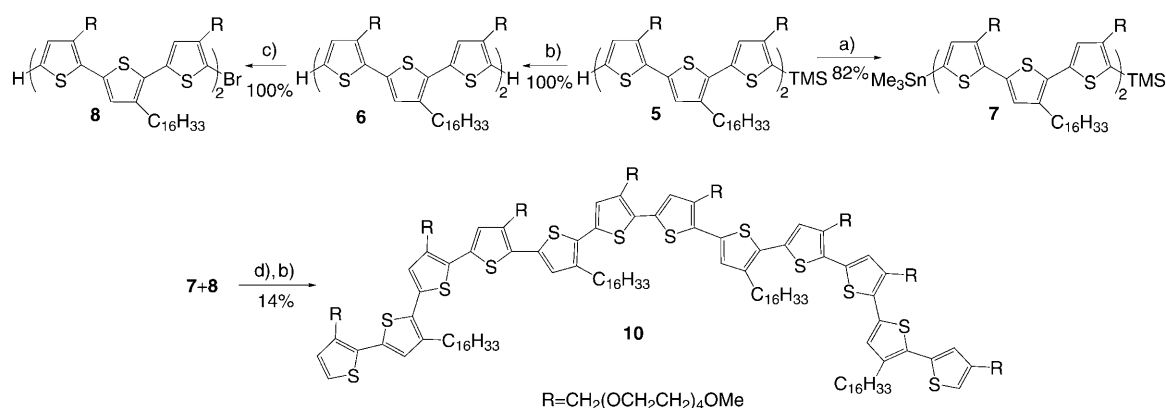
Amphiphilic terthiophene **1**, which was TMS-protected (TMS=trimethylsilane), was the starting compound from which the higher oligomers were formed (Scheme 3). Compound **1** was regioselectively converted to stannylated (**2**) and brominated (**4**) derivatives, which could then be connected by a Stille couplings to the regio-regular sexiathiophene **6**. First, **1** was *ortho*-lithiated by reaction with lithium diisopropylamide (LDA), followed by quenching with trimethyltin chloride, resulting in the introduction of a tin-moiety on the 5'''-position (**2**). Compound **4** was obtained in quantitative yield by first removal of the TMS-group from **1** by reaction with tetrabutyl ammonium fluoride (TBAF) to give **3**, followed by bromination on the 2-position with *N*-bromosuccinimide (NBS). A Stille coupling between **2** and **4** with  $[Pd(PPh_3)_4]$  gave the TMS-protected sexiathiophene **5** in 81% yield. Deprotection of **5** was performed again with TBAF in quantitative yield resulting in **6**.

The dodecathiophene oligomer **10** was synthesized following a similar approach as for **6** (Scheme 4). *ortho*-Lithiation and stannylation of **5** at the 5''''-position gave **7** in 82%



Scheme 3. Synthetic procedure for amphiphilic thiophene **6**: a) LDA,  $-78^\circ\text{C}$ ,  $Me_3SnCl$ ; b) TBAF, THF; c) NBS,  $CH_2Cl_2$ ; d)  $[Pd(PPh_3)_4]$ , DMF, toluene,  $110^\circ\text{C}$ .

yield and bromination of **6** afforded **8** in quantitative yield. A Stille cross-coupling of **7** and **8** gave the TMS-protected dodecamer **9**, which was directly deprotected to give **10** with an isolated yield of 14%. The isolated yield of the last coupling was significantly lower due to a combination of lower conversion and tedious purification. The compounds were purified by chromatography (normal, reverse phase, and size-exclusion (GPC)) and characterized using  $^1H$  and  $^{13}C$  NMR spectroscopy and mass spectrometry (electron



Scheme 4. Taking the same approach as for **6**, **10** was synthesized: a) LDA,  $-78^\circ\text{C}$ ,  $\text{Me}_3\text{SnCl}$ ; b) TBAF, THF; c) NBS,  $\text{CH}_2\text{Cl}_2$ ; d)  $[\text{Pd}(\text{PPh}_3)_4]$ , DMF, toluene,  $110^\circ\text{C}$ .

spray ionization (-ToF)). The purity of the compounds was confirmed by GPC (see the Supporting Information Figure SI1).

**Aggregation behavior of **3**, **6**, and **10** in water:** The oligothiophenes **3**, **6**, and **10** were readily soluble in water. Compounds **3** and **6** could be dissolved up to at least 90 and 50 mM giving clear yellow and orange solutions, respectively. The solution of **3** was clearly more viscous than water at concentrations from 1 mM, while solutions of **6** retained similar flow properties as water. The longest oligomer (**10**) was soluble up to at least 10 mM and at this concentration a dark red, highly viscous solution was formed, which was much more viscous than **3** at comparable concentrations. The increased viscosities of solutions of **3** and **10**, compared to a solution of **6** and water, clearly indicate the formation of different types of aggregates.

It is known that chromophores display changes in their photophysical properties upon aggregation<sup>[34]</sup> and therefore the absorption and emission properties of **3**, **6**, and **10** were studied in more detail. Remarkably, solutions of compound **3** and **10** in water exhibit no significant changes in both absorption and emission wavelengths over the concentration range from 0.005 to 10 mM. Only solutions of **6** in water displayed a shift of the maximum emission wavelength with increasing concentration. Because the expected effects of aggregation on the photophysical properties were not uniformly observed for all three compounds, it was necessary to study the self-assembly of **3**, **6**, and **10** by other methods. The photophysical properties will be discussed later. Unfortunately, surface tension measurements and isothermal titration calorimetry (ITC) were unsuitable to study the self-assembly behavior, because of surface tension instabilities and low enthalpies for dilution, respectively. The low enthalpies for dilution indicate that either self-assembly of the oligothiophene surfactants **3**, **6**, and **10** is a low-cooperative process and is mainly driven by entropy effects, or that the aggregates are highly stable and remain intact on the time scale of the ITC experiments (minutes).

The self-assembly of **3**, **6**, and **10** was established more firmly by dynamic light scattering (DLS) studies (Figure 2). From these measurements it appeared that the scattered light intensity for solutions of **3**, **6**, and **10** increased sharply at a specific concentration, which clearly indicates the formation of larger assemblies (Figure 2). The concentration of

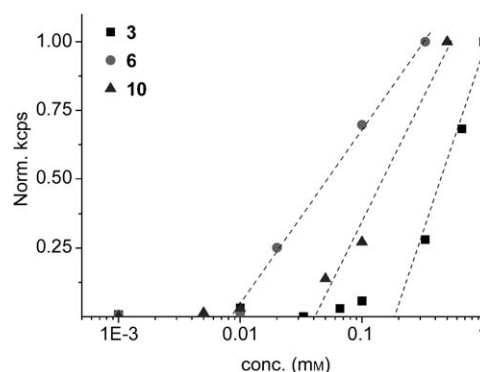


Figure 2. Number of counts (kilo-counts per second, kcps) for aggregates at different concentration of **3**, **6**, and **10**. When aggregates are formed, the counts increase drastically which is where the cmc is depicted. The added lines are solely a guide for the eye.

the sharp increase of the scattering intensity was taken as the critical micelle concentration (cmc), and the resulting values are summarized in Table 1. For all compounds the cmc values are below the millimolar regime, which is slightly above other tetraethyleneglycol surfactants with a hexadecyl chain.<sup>[35]</sup> The cmc of **6** and **10**, bearing more than one hexadecyl chain, is indeed lower than the cmc of **3**, but surprisingly, the cmc of **10**, bearing four alkyl chains, is slightly higher than the cmc of compound **6** with only two alkyl chains. The hydrodynamic diameter was investigated by DLS in separate measurements at concentrations above the cmc. All three compounds form assemblies with very different sizes. For **3**, a hydrodynamic diameter of 18 nm was found and this changes with concentration. The size is too large for a spherical micelle and an increasing diameter with

Table 1. Critical micelle concentration (cmc) determination by scattering and fluorescence.

	cmc <sub>DLS</sub> [mM] <sup>[a]</sup>	<i>D<sub>h</sub></i> [nm] <sup>[b]</sup>	cmc <sub>NR</sub> [mM] <sup>[c]</sup>
<b>3</b>	0.2	18	0.2
<b>6</b>	0.01	9	0.2
<b>10</b>	0.04	18, 91, 396	n.d.

[a] Determined cmcs by investigating the concentration dependent scattering by DLS. [b] The hydrodynamic diameter (*D<sub>h</sub>*) of 1.0 mM solutions of **3**, **6**, and **10**, estimated error 10%, values are taken as the number average. [c] Values for cmc of **3** and **6** obtained using fluorescence in combination with Nile Red ( $\lambda_{\text{exc}}$ : 550 nm) by investigating the change in emission intensity. Estimated error in cmc is  $\approx 10\%$ . Experiments were performed at 20°C.

increasing concentration suggests elongated micelles, which is in agreement with the observed visco-elastic properties of the solution. The hydrodynamic diameter found for **6** was 9 nm and did not show any concentration dependency. The size would be appropriate for spherical micelles. Compound **10** displayed a polydisperse distribution of the hydrodynamic radii varying between 18 and 400 nm (see Table 1). Moreover, they strongly depend on the concentration of **10**.

The nature of the assemblies formed by **3**, **6**, and **10** was further investigated by studying the emission properties of Nile Red, which is a known fluorescent probe for hydrophobic domains. The fluorescence intensity of Nile Red will increase when it is located in hydrophobic domains, formed during aggregation, and also the emission maximum ( $\lambda_{\text{em}}$ ) will shift towards the blue ( $\lambda_{\text{em}}(\text{NR}) = 660$  nm in water). The emission intensity of Nile Red showed a clear increase at concentrations around 0.2 mM for both **3** and **6** (Table 1 and Figure SI2 in the Supporting Information), which for **6** is at a significantly higher concentration than the cmc value determined by light scattering. However, when looking at the shift in  $\lambda_{\text{em}}(\text{NR})$ , it was observed that, already at micromolar concentrations of oligothiophene, a significant shift has occurred towards 640 and 622 nm (see Figure SI2 in the Supporting Information) for **3** and **6**, respectively. This indicates that hydrophobic domains are already formed well below their respective cmcs, presumably due to the formation of pre-aggregates. Though Nile Red is known to induce aggregation,<sup>[36]</sup> the formation of pre-aggregates was also observed in a previous study with different terthiophene amphiphiles and concurs with fluorescence measurements without Nile Red.<sup>[37]</sup> For **10**, the cmc could not be determined with Nile Red because of nonselective excitation due to overlap of the absorption spectra of Nile Red and **10**. No other fluorescent probe was found to have its excitation outside the absorption range of **10**.

The thiophene amphiphiles **3**, **6**, and **10** have oligoethylene glycol moieties as hydrophilic groups, and therefore they might exhibit a cloudpoint (cp).<sup>[35,38]</sup> Oligothiophene surfactants **3** and **6** exhibit well-defined cloudpoints of 26°C and 38°C, respectively, while for compound **10** no cloudpoint was observed between 5 and 90°C.

**Morphology of aggregated 3, 6, and 10 in water:** The values of the hydrodynamic diameter listed in Table 1 and the dif-

ferences in visco-elastic properties of solutions of **3**, **6**, and **10** already suggested assemblies with different morphologies. To elucidate these different properties, the morphologies of the aggregates of **3**, **6**, and **10** were investigated using cryo-transmission electron microscopy (TEM). For all cryo-TEM studies described below, samples were prepared by quenching 10 mM solutions of **3**, **6**, and **10** in water from 20°C, that is, well above the critical micelle concentration and well below the cloudpoint. The diameters of the different aggregate morphologies were determined by measuring one hundred different positions on several aggregates and several electron-micrographs, from which the average was taken.

The cryo-TEM studies revealed that the amphiphilic oligothiophenes **3**, **6**, and **10** clearly formed different morphologies upon self-assembly in water (Figure 3). For compound

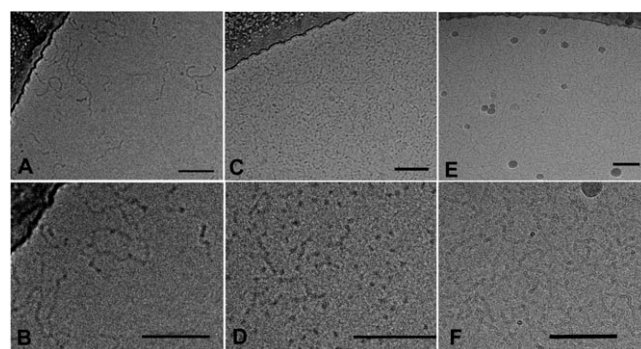


Figure 3. Cryo-transmission electron micrographs of the **3** showing elongated micelles (A and B), **6** showing clustered spherical aggregates (C and D), **10** showing tubular like elongated micelles (E and F), the scale bar notes 100 nm.

**3**, elongated micelles were observed with a diameter of  $7.1 \pm 1.0$  nm, and a contour length of about 100–150 nm (Figure 3A, B). This last value is a crude estimate, since the structures are coiling and overlap in the micrograph at these relatively high concentrations. The presence of elongated micelles explains the visco-elastic properties of the solution, and also concurs with the previously mentioned DLS measurements. The TEM images of compound **6** displayed spherical micelles with a diameter of about  $7.4 \pm 0.9$  nm (Figure 3C, D). This is smaller than the hydrodynamic diameter of 9 nm measured by DLS, but this value also includes the hydration shell. When looking carefully, the aggregates tend to cluster into elongated structures with the individual spherical structures still visible. The cryo-TEM images of solutions of compound **10** displayed dense network of cylindrical micelles, which is in excellent agreement with the observed viscoelastic properties of the solutions. The diameter of the cylindrical micelles of **10** amounted to  $5.4 \pm 0.8$  nm, but the contour length could not be determined due to extreme overlap of the structures (Figure 3E, F). These observations nicely explain the polydispersity as observed by DLS.

Even though at first sight the aggregate morphologies are similar to comparable aggregate morphologies formed by

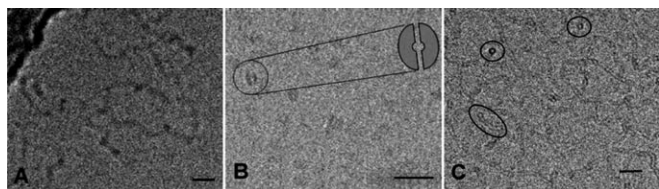


Figure 4. Cryo-transmission electron micrographs, highly magnified in order to show the contrast differences and displaying a difference fine structure in the aggregates between **3** A), **6** B) and **10** C). Scale bar depicts 20 nm.

other more common surfactants, when taking a closer look at the fine structure some striking features emerged (Figure 4). The aggregates formed by compound **3** looks just like what one would expect from an elongated micelle: an elongated structure with a homogeneous filling and a darkening at the ends due to a higher density of surfactants. When enlarging the structures of **6**, it became visible that the contrast is not equally distributed throughout the aggregate. In the middle there is a clear spot which has less contrast and it appears as if there is a structure of increased density at the edges.

Similar contrast differences were observed for the aggregates of **10**. For these structures, the contrast was higher along the long edges of the elongated structure, and also many circular structures with strongly enhanced contrast at the edges were visible. These elongated and circular structures are most likely the longitudinal and cross section of a tubular, perhaps intertwined structure, respectively. At this point it is not known what the origins of the fine structure are, but this is currently under investigation.

The observed diameters of aggregates of **3**, **6**, and **10** deviate significantly. For **3** and **6** the diameter determined by cryo-TEM amounted to 7.1 and 7.4 nm, respectively. When taking into account the dimensions of the surfactant, which can be seen as a flat triangular shape, the total area of the surfactant ( $\sigma$  (m<sup>2</sup>)) and the full width of the triangular shape ( $\delta$  (m)) of the surfactant, compounds **3** and **6** can also be described by a conventional packing<sup>[1,39]</sup> with an approximate diameter calculated according to Equation (2).

$$D = \frac{4\sigma}{\delta} \quad (2)$$

It should be noted that here the assumption is made that the side-chains are in their fully extended state which is not accurate for most systems bearing long flexible chains. It was found that for **3** and **6** the diameter approximated by Equation (2) amount to 8.0 and 8.4 nm, respectively. Within 10–15% error margin, the values are the same as the measured values and also show that indeed **6** should have a slightly larger diameter than **3**. When the same determination of diameter is applied to compound **10**, a diameter of 8.4 nm was found, the same as for **6**. However, experimentally the diameter was about 35% smaller, 5.4 nm.

The findings suggest that the morphology of **10** does not follow conventional packing. Common micelle forming sur-

factants are said to have a cone shaped molecular structure, while the amphiphiles used here are flat. This will already influence the molecular packing inside the aggregates. Since the different oligomers are of similar design with an equal ratio of hydrophilic and hydrophobic groups, one would normally expect similar aggregate morphologies should be formed. It can be concluded from this that the curvature also influences the packing of the surfactants since this is the main difference between the structures shown here.

The molecular curvature is located along the oligothiophene backbone and the diameter of this circular structure is 5.4 nm. However, the aliphatic chains are about 2.0 nm in length. This means that only a cross section of 4.0 nm can be filled inside the hydrophobic domain of the micellar structure. This would result in an empty space upon aggregation, which is not desirable, and as a result the system finds another type of packing. Some possible packings of the oligothiophene surfactants are depicted in Figure 5.

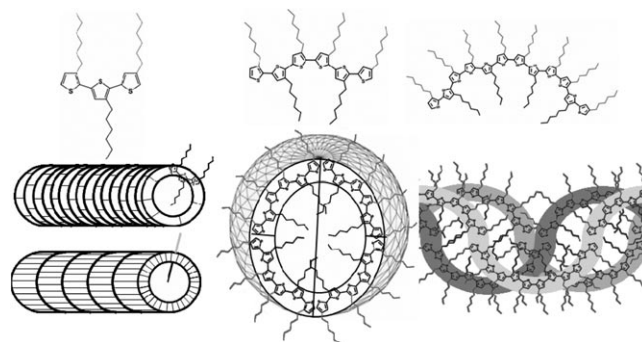


Figure 5. Suggested packing of compounds **3**, **6**, and **10** in their aggregated form in water. Elongated micelles with either a face-to-face or edge-to-edge packing and spherical micelles are observed for **3** and **6**, respectively. For **10** a different packing is suggested, more intertwined which causes the reduced diameter and explains the fine structure observed in Figure 4C.

Here **3** can potentially pack in two ways, either with the thiophene backbone parallel or perpendicular to the long axis of the elongated micelle. The aggregate of compound **6** is spherical in nature and therefore will pack in such a way that the surface curvature of the aggregate extends in two directions in the same structure. The surfactants are oriented at a certain angle with respect to each other to obtain the spherical structure. For **10**, a completely different approach is necessary in order to obtain the reduced diameter. Intertwining of the curved surfactant is a way that they can form aggregates with a significant smaller diameter than initially was predicted. This intertwining is also a possible cause of the fine structure that was presented in Figure 4C.

**Photophysical properties of 3, 6, and 10:** It was expected that the intrinsic photo-physical properties of the oligothiophenes **3**, **6**, and **10** could be exploited to derive information about their self-assembly behavior. As already noted above, the aggregation of **3** and **10** in water, however, was not ac-



Table 2. Photophysical properties of **3**, **6**, and **10** in water and chloroform.

	$\lambda_{\text{abs}}^{[a]}$ (H <sub>2</sub> O) [nm]	$\lambda_{\text{em}}^{[a]}$ (H <sub>2</sub> O) [nm]	$\epsilon^{[a]}$ [10 <sup>3</sup> L mol <sup>-1</sup> cm <sup>-1</sup> ]	$\lambda_{\text{abs}}^{[a]}$ (CHCl <sub>3</sub> ) [nm]	$\lambda_{\text{em}}^{[a]}$ (CHCl <sub>3</sub> ) [nm]	$\epsilon^{[a]}$ [10 <sup>3</sup> L mol <sup>-1</sup> cm <sup>-1</sup> ]	$\Delta E_{\text{abs}}^{[b]}$ [eV] (CHCl <sub>3</sub> /H <sub>2</sub> O)	$\text{cac}_{\text{PL}}^{[c]}$ [mM]
<b>3</b>	348	461	16.2	337	444	26.2	0.11	0.1
<b>6</b>	423	572	35.7	404	523	35.0	0.14	0.01
<b>10</b>	454	645	69.4	426	564	77.6	0.17	0.01

[a] Concentrations used were 1.0 mM for **3** and 0.1 mM for **6** and **10**. Listed are the  $\lambda_{\text{max}}$  for absorption and emission, the molar absorption coefficient ( $\epsilon$ ) in water and chloroform. [b] Also listed is the energy difference in eV of the  $\lambda_{\text{max}}$  for absorption between both solvents to depict the amount of created disorder between a discriminating to a nondiscriminating solvent. [c] The concentration at which the photoluminescence (PL) deviates from linearity with increasing concentration. Estimated error in cac is  $\approx 10\%$ .

accompanied by significant changes of the absorption and emission maxima.<sup>[40]</sup> Solutions of compound **6** displayed a clear shift of the emission maxima of 51 nm towards the blue, upon increasing the concentration above 0.03 mM (Figure SI3 in the Supporting Information). This concentration is in good agreement with the cmc determined by DLS. It was, however, observed that the emission intensity did not increase linearly with the concentration of **3**, **6**, and **10** and even at some point decreased, most likely due to self-quenching caused by aggregation of the compounds.<sup>[41]</sup>

This fluorescence self-quenching occurred already at much lower concentrations than the cmc values determined with Nile Red emission intensity and light scattering, but does occur at similar concentrations when compared to the concentrations at which the Nile Red emission wavelength shifts (for **3** and **6**). For compounds **3**, **6**, and **10** self-quenching started at concentrations of 0.1, 0.01 and 0.01 mM, respectively (Figure SI3 in the Supporting Information and Table 2). Most likely, the self-quenching occurring below the cmc is due to the formation of small pre-micellar aggregates. The formation of these aggregates has been reported before for other systems.<sup>[37,42]</sup> The onset of the self-quenching gives information about the concentration at which monomeric surfactants in solution start to aggregate, that is, the critical aggregation concentration (cac).

Water is a discriminating solvent for the amphiphiles since one part of the amphiphile does not want to dissolve while the other part does. This induces a certain orientation of the groups, influencing the position of the thiophenes and their planarity. When both types of chains (aliphatic and hydrophilic) extend to opposite sides, the thiophenes will be planar and, in the case of **6** and **10**, also curved. In a nondiscriminating solvent both chains are soluble and therefore, even though the all-*trans* configuration would be preferred, will have some more rotational freedom over the thiophene–thiophene bonds. The difference between the rigid curved conformation and all-*trans* configuration with more rotational freedom was observed in the photophysical properties as the conformation is directly related to the conjugation length which can be observed in the absorption maximum. When a discriminating solvent (H<sub>2</sub>O) and a nondiscriminating solvent (CHCl<sub>3</sub>) are compared, it is seen that in CHCl<sub>3</sub> there is a shift in the absorption towards the blue, which can be interpreted as a reduction in conjugation length. This was also reflected in the emission (Table 2, Figure 6) for which a similar trend was observed. This

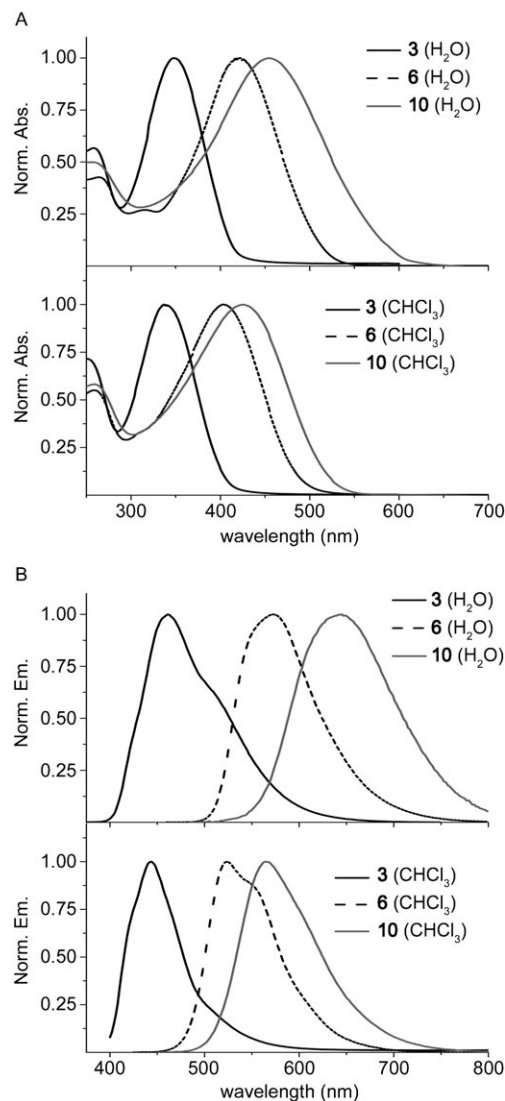


Figure 6. A) Absorption and B) emission spectra in water (top) and chloroform (bottom). Spectra were taken at concentrations of 1.0 mM for **3** and 0.1 mM for **6** and **10**. Large blue shifts are observed when compared between water and chloroform. The values for the  $\lambda_{\text{max}}$  of emission and absorption are listed in Table 2. Measurements were performed at 20 °C and excitation was done at the corresponding absorption maximum.

change could also be interpreted as interactions between adjacent chromophores in an aggregated state that have electronic interactions. However, although for **6** such a transition in aggregation could be observed in the emission, it did



not result in a change in the absorption. Also similar changes in absorption have been reported going from a disordered to an ordered conformation without aggregation.<sup>[32]</sup> Most likely, self-assembly of these oligothiophenes, and especially the longer **6** and **12**, is accompanied by a transition from a disordered conformation towards a more planar conformation with increased conjugation between thiophene moieties. It should be noted that also other effects, for instance exciton coupling between chromophores and solvent polarity, are likely to contribute to the large shifts observed in water compared to  $\text{CHCl}_3$ , and therefore this conclusion remains tentative.

## Conclusion

In this study the possibility to control the size and shape of self-assembled structures through the local curvature of their molecular building blocks has been investigated. To this end a series of amphipathic conjugated oligothiophenes with a well-defined curvature of their backbone has been designed and synthesized. The molecular (local) curvature of these oligothiophenes resulted from a preference for *cis* instead of *trans* conformations at specific positions along the oligothiophene backbone, which can be controlled by the sequence of hydrophilic and hydrophobic groups, while their ratio constant was kept constant. It was found that the morphology depends on the length of the oligomers. The structure–morphology relationship of terthiophene **3** and sexi-thiophene **6** could be described by conventional packing theory, but the diameter for aggregates of dodecathiophene **10** deviated significantly from predicted diameters. The different behavior of **10** can be interpreted as a more pronounced expression of the local curvature of this dodecathiophene.

The self-assembly of oligothiophenes **3**, **6**, and **10** appeared to be a low-cooperative process, involving the formation of premicellar aggregates at sub-millimolar concentrations, which at concentrations in the millimolar regime transformed into micelles and cylindrical micelles. Unfortunately, the occurrence of pre-micellar aggregates obscured aggregation-dependent changes of the photophysical properties, which precluded the use of such changes as a intrinsic reporter for self-assembly behavior and aggregate structure. A comparison with the photophysical properties in a non-aggregating solvent, however, suggested that aggregation of especially the longer oligothiophenes is accompanied by a transition to a more planar conformation.

These observations demonstrate that the aggregation morphology of simple amphipathic oligothiophenes can be controlled by the implementation of an additional structural motif namely, the curvature. Currently it is under investigation whether this can be extended, thereby developing a new approach to predicting and designing aggregate morphologies with specific diameters derived from the intrinsic molecular curvature. This class of conjugated curved amphipathic molecules has potential functions in aqueous elec-

tronic devices as sensors and light harvesting systems but also they would be compatible with biological systems like living cells.

## Experimental Section

**General information:** Starting materials were commercially available and were used without further purification. Synthesis of compound **1** has been described previously.<sup>[42]</sup> Aldrich silica gel Merck grade 9385 (230–400 mesh) was used for column chromatography, in combination with the Teledyne Isco CombiFlash Companion with UV detection. All solvents used for dry reactions were purified with the use of MBRAUN Solvent purification system MB SPS-800. MilliQ-water and spectroscopic grade solvents were used for measurements.  $^1\text{H}$  NMR spectra were recorded on a Bruker Avance-400 spectrometer (at 400 MHz) or a Varian Inova-300 spectrometer (at 300 MHz), at 25 °C. The splitting patterns are noted as follows: s (singlet), d (doublet), dd (double doublet), t (triplet), q (quartet), qt (quintet), m (multiplet) and brs (broad singlet).  $^{13}\text{C}$  NMR spectra were recorded on a Bruker Avance-400 spectrometer (at 100 MHz) or a Varian Inova-300 spectrometer (at 75 MHz). Multiplicity was determined by attached proton test (APT) and chemical shifts are given in  $\delta$  (ppm) referenced to the residual protic solvent peaks. Coupling constants  $J$ , are given in Hz. GPC was performed on a Waters gel permeation chromatography machine, LC-8 A pump with a Waters dual  $\lambda$  absorbance detector (detection wavelength set on 254 and 360 nm). The column used here was the reprogel PS-GPC 500, 5  $\mu\text{m}$  particle size dimensions  $300 \times 30$  mm for preparative with a  $6 \text{ mL min}^{-1}$  flow and 2.5 mL injection volume, for analytical the same column with dimensions  $30 \times 8$  mm was used with a flow of  $1 \text{ mL min}^{-1}$  (THF) with 50  $\mu\text{L}$  injection volume. Surface Tension measurements were done on a setup by KRÜSS FM40 Easy Drop, consisting of a syringe pump and a CCD camera, at ambient temperature. Isothermal titration calorimetry was done on a Microcal VP-ITC micro-calorimeter apparatus at 20 °C. For UV/Vis measurements an AnalytikJena Specord 250 spectrometer was used equipped with a deuterium-lamp and a halogen-lamp. Quartz cuvettes were used with path-lengths varying from 10–0.1 mm. Fluorescence spectroscopy was done on a Jasco J-815 CD-spectrometer equipped with a fluorescence monochromator and detector, and an L-38 low wavelength filter (cut-off 380 nm) placed between the sample and the detector. The cuvet used here was quartz with dimensions  $3 \times 3$  mm. Dynamic light scattering was performed on a ZetaSizer Nano series Nano-ZS by Malvern Instruments at 20 °C. For cryo-TEM, a few microliter of suspension was deposited on a bare 700 mesh copper grid. After blotting away the excess of liquid the grids were plunged quickly in liquid ethane. Frozen-hydrated specimens were mounted in a cryo-holder (Gatan, model 626) and observed in a Philips CM 120 electron microscope, operating at 120 kV. Micrographs were recorded under low-dose conditions on a slow-scan CCD camera (Gatan, model 794).

**Preparation of compound 2:** A solution of diisopropylamine (0.5 mL) in anhydrous THF (20 mL) was cooled to  $-78^\circ\text{C}$ . *n*-Butyllithium (1.75 mL, 2.8 mmol; 1.6 M in hexane) was then added to the solution. The mixture was then allowed to reach  $0^\circ\text{C}$  and was stirred at this temperature for 10 min. Then it was again cooled to  $-78^\circ\text{C}$  and a solution of **1** (2.6 g, 2.6 mmol) in dry THF (30 mL) was added and the mixture was stirred for 4 h at  $-78^\circ\text{C}$ . Then a solution trimethyltinchloride (5 mL; 1 M in THF) was added and the mixture was further stirred at  $-78^\circ\text{C}$ . After 3 h the reaction mixture was allowed to slowly warm to room temperature overnight. The mixture was quenched with water and extracted with  $\text{CH}_2\text{Cl}_2$ . The organic phase was dried over  $\text{MgSO}_4$  and the solvent was removed in vacuo. Compound **2** was obtained as a yellow oil in 89% yield (2.7 g, 2.4 mmol). This compound was used without further purification.  $^1\text{H}$  NMR (400 MHz,  $\text{CDCl}_3$ ):  $\delta$  = 0.37 (s, 9H), 0.38 (t,  $J^{\text{sn}}$  = 24.0 Hz, 9H), 0.88 (t,  $J_3$  = 7.4 Hz, 3H), 1.15–1.40 (m, 26H), 1.60–1.68 (m, 2H), 2.75 (t,  $J_3$  = 7.8 Hz, 2H), 3.37 (s, 6H), 3.54–3.63 (m, 4H), 3.66–3.76 (m, 28H), 4.56 (s, 2H), 4.64 (s, 2H), 6.98 (s, 1H), 7.18 (s, 1H), 7.20 ppm (s, 1H).

**Preparation of compound 3:** A solution of TBAF (10 mL; 1.0 M in THF) was added to a solution of compound **1** (2.6 g, 2.6 mmol) in THF (10 mL) and the resulting mixture was stirred overnight. After removal of the solvent the yellow oil was dissolved in water and of cationic ion-exchange resin (DOWEX MAC-3; ca. 100 g) was added and the suspension was stirred until the water became colourless and the resin yellow. This was then filtrated and washed several times with water to remove the TBAF. After extensive rinsing, the product was released from the resin by washing with methanol to obtain pure compound **3** as a yellow oil in quantitative yield (2.4 g, 2.6 mmol). <sup>1</sup>H NMR (400 MHz, CDCl<sub>3</sub>): δ = 0.87 (t, J<sub>3</sub> = 7.4 Hz, 3H), 1.15–1.40 (m, 26H), 1.60–1.68 (m, 2H), 2.73 (t, J<sub>3</sub> = 7.8 Hz, 2H), 3.37 (s, 6H), 3.54–3.63 (m, 4H), 3.66–3.76 (m, 28H), 4.55 (s, 2H), 4.64 (s, 2H), 6.99 (s, 1H), 7.08 (d, J<sub>4</sub> = 1.3 Hz, 1H), 7.12 (d, J<sub>3</sub> = 5.2 Hz, 1H), 7.19 (d, J<sub>3</sub> = 5.6 Hz, 1H), 7.20 ppm (d, J<sub>4</sub> = 1.3 Hz, 1H); <sup>13</sup>C NMR (100 MHz, CDCl<sub>3</sub>): δ = 13.99 (CH<sub>3</sub>), 22.50 (CH<sub>2</sub>), 29.10 (CH<sub>2</sub>), 29.17 (CH<sub>2</sub>), 30.45 (CH<sub>2</sub>), 31.53 (CH<sub>2</sub>), 61.56 (CH<sub>2</sub>), 66.77 (CH<sub>2</sub>), 68.42 (CH<sub>2</sub>), 69.30 (CH<sub>2</sub>), 69.33 (CH<sub>2</sub>), 70.18 (CH<sub>2</sub>), 70.44 (CH<sub>2</sub>), 70.47 (CH<sub>2</sub>), 70.50 (CH<sub>2</sub>), 72.45 (CH<sub>2</sub>), 122.84 (CH), 123.85 (CH), 126.04 (CH), 129.20 (CH), 130.03 (CH), 132.98 (C), 134.99 (C), 136.13 (C), 139.64 (C), 140.06 ppm (C); purity analyzed by GPC (UV/Vis): t<sub>R</sub> = 507 s; MS: m/z calcd for C<sub>48</sub>H<sub>314</sub>O<sub>4</sub>S<sub>12</sub>: 912.49 (mono-isotopic); found: 935.5 [M+Na]<sup>+</sup>.

**Preparation of compound 4:** N-Bromosuccinimide (0.5 g, 2.8 mmol) was added to a solution of **3** (2.4 g, 2.6 mmol) in CH<sub>2</sub>Cl<sub>2</sub> (100 mL). The mixture was stirred overnight, followed by removal of the solvent in vacuo. The crude product was dissolved in cold heptane and filtered over celite. After evaporation of the heptane, pure compound **4** was obtained as a yellow oil in quantitative yield (2.6 g, 2.6 mmol). <sup>1</sup>H NMR (400 MHz, CDCl<sub>3</sub>): δ = 0.87 (t, J<sub>3</sub> = 7.4 Hz, 3H), 1.15–1.40 (m, 26H), 1.60–1.68 (m, 2H), 2.67 (t, J<sub>3</sub> = 8.0 Hz, 2H), 3.34 (s, 6H), 3.49–3.54 (m, 4H), 3.58–3.68 (m, 28H), 4.48 (s, 2H), 4.60 (s, 2H), 6.97 (s, 1H), 6.99 (s), 7.10 (d, J<sub>3</sub> = 5.2 Hz, 1H), 7.17 ppm (d, J<sub>3</sub> = 5.2 Hz, 1H).

**Preparation of compound 5:** A solution of **4** (2.4 g, 2.4 mmol) and palladium(tetrakis)triphenylphosphine (1.0 g, 0.9 mmol) in DMF/toluene (20 mL; 50:50) was prepared under a nitrogen atmosphere and stirred for 20 min. A solution of **2** (2.7 g, 2.4 mmol) in DMF/toluene (5 mL; 50:50) was added and the resulting mixture was heated at 110 °C overnight. The solvent of the reaction mixture was removed in vacuo and the crude product was purified by column chromatography (reverse phase C18-silica, flushing with acetonitrile removed impurities, flushing with CH<sub>2</sub>Cl<sub>2</sub> gave pure compound). This gave pure compound **5** as a red oil in 81 % yield (3.6 g, 1.9 mmol). <sup>1</sup>H NMR (400 MHz, CDCl<sub>3</sub>): δ = 0.36 (s, 9H), 0.85 (t, J<sub>3</sub> = 7.4 Hz, 6H), 1.15–1.40 (m, 52H), 1.60–1.68 (m, 4H), 2.75 (m, J<sub>3</sub> = 7.8 Hz, 4H), 3.32–3.38 (m, 12H), 3.54–3.63 (m, 8H), 3.66–3.76 (m, 56H), 4.55 (s, 2H), 4.64 (brs, 6H), 6.99 (s, 1H), 7.03 (s, 1H), 7.11 (d, J<sub>3</sub> = 5.2 Hz, 1H), 7.15 (s, 1H), 7.17 (d, J<sub>3</sub> = 5.2 Hz, 1H), 7.19 (s, 1H), 7.21 ppm (s, 1H).

**Preparation of compound 6:** Compound **5** (0.74 g, 0.39 mmol) was stirred overnight in 10 mL THF with added, 0.5 mL of a 1.0 M TBAF solution in THF. After removal of the solvent the red oil was dissolved in water and about 100 g of cationic ion-exchange resin (DOWEX MAC-3) was added and the suspension was stirred until the water became colorless and the resin red. This was then filtrated and washed several times with water to remove the TBAF. After extensive rinsing, the product was released from the resin by washing with THF to obtain the pure title compound as a red oil in quantitative yield (0.71 g, 0.39 mmol). <sup>1</sup>H NMR (400 MHz, CDCl<sub>3</sub>): δ = 0.87 (t, J<sub>3</sub> = 7.4 Hz, 6H), 1.15–1.40 (m, 52H), 1.60–1.68 (m, 4H), 2.75 (m, J<sub>3</sub> = 7.8 Hz, 4H), 3.32–3.38 (m, 12H), 3.54–3.63 (m, 8H), 3.66–3.76 (m, 56H), 4.55 (s, 2H), 4.63 (s, 2H), 4.64 (brs, 4H), 7.00 (s, 1H), 7.04 (s, 1H), 7.09 (s, 1H), 7.13 (d, J<sub>3</sub> = 5.2 Hz, 1H), 7.15 (s, 1H), 7.18 (d, J<sub>3</sub> = 5.2 Hz, 1H), 7.20 ppm (brs, 2H); <sup>13</sup>C NMR (75 MHz, CDCl<sub>3</sub>): δ = 14.06 (CH<sub>3</sub>), 22.62 (CH<sub>2</sub>), (CH<sub>3</sub>), 29.30 (CH<sub>2</sub>), 29.61 (CH<sub>2</sub>), 29.66 (CH<sub>2</sub>), 31.86 (CH<sub>2</sub>), 66.88 (CH<sub>2</sub>), 68.52 (CH<sub>2</sub>), 69.42 (CH<sub>2</sub>), 69.55 (CH<sub>2</sub>), 70.54 (CH<sub>2</sub>), 70.59 (CH<sub>2</sub>), 71.87 (CH<sub>2</sub>), 122.89 (CH), 123.94 (CH), 126.10 (CH), 128.52 (CH), 129.35 (CH), 130.12 (CH), 130.69 (C), 131.52 (C), 132.52 (C), 132.87 (C), 133.23 (C), 133.28 (C), 133.83 (C), 134.15 (C), 134.64 (C), 135.22 (C), 135.58 (C), 135.66 (C), 136.11 (C), 139.83 (C), 140.30 (C), 140.40 ppm (C); purity analyzed by GPC (UV/Vis): t<sub>R</sub> =

485 s; MS: m/z calcd for C<sub>96</sub>H<sub>158</sub>O<sub>20</sub>S<sub>6</sub>: 1822.97 (mono-isotopic); found: 930.2 [M+2NH<sub>4</sub>]<sup>2+</sup>; 932.5 [M+Na+NH<sub>4</sub>]<sup>2+</sup>.

**Preparation of compound 7:** A solution of diisopropylamine (0.15 mL) in anhydrous THF (5 mL) was cooled to –78 °C. n-Butyllithium (0.22 mL, 0.35 mmol; 1.6 M in hexane) was then added. The mixture was then allowed to reach 0 °C and was stirred at this temperature for 10 min. Then it was again cooled to –78 °C and a solution of **5** (0.66 g, 0.35 mmol) in dry THF (10 mL) was added and the mixture was stirred for 4 h at –78 °C. Then a solution of trimethyltinchloride (0.5 mL, 1 M in THF) was added and the mixture was further stirred at –78 °C. After 3 h the reaction mixture was allowed to slowly warm to room temperature overnight. The mixture was quenched with water and extracted with CH<sub>2</sub>Cl<sub>2</sub>. The organic phase was dried over MgSO<sub>4</sub> and the solvent was removed in vacuo. Compound **7** was obtained as a red oil in 82 % yield 0.58 g (0.28 mmol). This compound was used without further purification. <sup>1</sup>H NMR (300 MHz, CDCl<sub>3</sub>): δ = 0.36 (s, 9H), 0.38 (s, 9H), 0.85 (t, J<sub>3</sub> = 7.4 Hz, 6H), 1.15–1.40 (m, 52H), 1.60–1.68 (m, 4H), 2.78 (m, J<sub>3</sub> = 7.8 Hz, 4H), 3.32–3.38 (m, 12H), 3.54–3.63 (m, 8H), 3.66–3.76 (m, 56H), 4.57 (s, 2H), 4.64 (brs, 6H), 7.03 (s, 1H), 7.08 (s, 1H), 7.16 (s, 1H), 7.19 (d, J<sub>3</sub> = 5.2 Hz, 1H), 7.21 (s, 1H), 7.22 ppm (s, 1H).

**Preparation of compound 8:** N-bromosuccinimide (0.07 g, 0.4 mmol) was added to a solution of **6** (0.69 g, 0.38 mmol) in CH<sub>2</sub>Cl<sub>2</sub> (10 mL). The mixture was stirred overnight. After completion the solvent was removed in vacuo. The crude was solubilised in cold heptane and filtered over celite. After the evaporation of heptane, compound **8** was obtained in quantitative yield as a red oil (0.72 g, 0.38 mmol) was obtained. <sup>1</sup>H NMR (400 MHz, CDCl<sub>3</sub>): δ = 0.85 (t, J<sub>3</sub> = 7.4 Hz, 6H), 1.15–1.40 (m, 52H), 1.60–1.68 (m, 4H), 2.75 (m, J<sub>3</sub> = 7.8 Hz, 4H), 3.32–3.38 (m, 12H), 3.54–3.63 (m, 8H), 3.66–3.76 (m, 56H), 4.55 (s, 2H), 4.64 (brs, 6H), 7.01 (s, 1H), 7.02 (s, 1H), 7.04 (s, 1H), 7.17 (d, J<sub>3</sub> = 5.2 Hz, 1H), 7.18 (s, 1H), 7.21 (d, J<sub>3</sub> = 5.2 Hz, 1H), 7.22 ppm (s, 1H).

**Preparation of compound 10:** A solution of **8** (0.70 g, 0.37 mmol) and palladium(tetrakis)triphenylphosphine (0.2 g, 0.2 mmol) in DMF/toluene (10 mL 50:50) was prepared under a nitrogen atmosphere and stirred for 20 min. A solution **7** (0.58 g, 0.28 mmol) in DMF/toluene (50/50) was added and the resulting mixture was heated at 110 °C overnight. The solvent of the reaction mixture was removed in vacuo and the crude was purified by column chromatography (reverse phase C18-silica, flushing with acetonitrile removes impurities, flushing with CH<sub>2</sub>Cl<sub>2</sub> gives mixture of compounds, that is, compound **9**, starting materials, and side-products. It was chosen first to remove the TMS group and then continue purification in order to minimize the number of possible compounds. To this extent crude **9** (1.3 g) was stirred overnight in a solution of TBAF (0.5 mL, 1.0 M solution in THF) in THF (10 mL). After removal of the solvent the dark red oil was dissolved in water and a cationic ion-exchange resin (DOWEX MAC-3) was added and the suspension was stirred until the water became colorless and the resin red. This was then filtrated and washed several times with water to remove the TBAF. After extensive rinsing, the product was released from the resin by washing with THF to obtain 1.0 g crude product as a dark red oil after removal of the solvent. The crude product was purified by GPC (Repro-Gel PS, 5 μm, 500 Å, THF), which allowed isolation of compound **10** as a dark red oil, in 14 % yield (150 mg, 0.04 mmol). <sup>1</sup>H NMR (400 MHz, CDCl<sub>3</sub>): δ = 0.87 (t, J<sub>3</sub> = 7.4 Hz, 12H), 1.15–1.40 (m, 104H), 1.60–1.68 (m, 8H), 2.79 (brs, 8H, J<sub>3</sub> = 7.8 Hz), 3.32–3.38 (m, 24H), 3.54–3.63 (m, 16H), 3.66–3.76 (m, 112H), 4.56 (s, 2H), 4.61–4.69 (brs, 14H), 7.01 (s, 1H), 7.05 (s, 1H), 7.07 (s, 1H), 7.09 (s, 1H), 7.14 (d, J<sub>3</sub> = 5.2 Hz, 1H), 7.16–7.24 ppm (overlapping thiophene protons, 9H); <sup>13</sup>C NMR (75 MHz, CDCl<sub>3</sub>): δ = 14.06 (CH<sub>3</sub>), 22.62 (CH<sub>2</sub>), (CH<sub>3</sub>), 29.30 (CH<sub>2</sub>), 29.61 (CH<sub>2</sub>), 29.66 (CH<sub>2</sub>), 31.86 (CH<sub>2</sub>), 66.88 (CH<sub>2</sub>), 68.52 (CH<sub>2</sub>), 69.42 (CH<sub>2</sub>), 69.55 (CH<sub>2</sub>), 70.54 (CH<sub>2</sub>), 70.59 (CH<sub>2</sub>), 71.87 (CH<sub>2</sub>), 128–142 ppm (clusters of overlapping signals of 14 CH and 34 C); purity analyzed by GPC (UV/Vis): t<sub>R</sub> = 438 s; ESI-TOF: m/z calcd for C<sub>192</sub>H<sub>314</sub>O<sub>40</sub>S<sub>12</sub>: 3643.92 (mono-isotopic) found: 1844.9081 [M+2Na]<sup>2+</sup> 1237.6293 [M+3Na]<sup>3+</sup>, calculated from this gives Mw: 3643.8 (mono-isotopic).

## Acknowledgements

Dr. G.J.M. Koper is kindly acknowledged for helpful discussions. This work was funded by the Netherlands Organization for Scientific Research (NWO).

- [1] a) I. W. Hamley, V. Castelletto, *Angew. Chem.* **2007**, *119*, 4524–4538; *Angew. Chem. Int. Ed.* **2007**, *46*, 4442–4455; b) A. J. Kirby, P. Camilleri, J. B. F. N. Engberts, M. C. Feiters, R. J. M. Nolte, O. Söderman, M. Bergsma, P. C. Bell, M. L. Fielden, C. L. García Rodríguez, P. Guédat, A. Kremer, C. McGregor, C. Perrin, G. Ronsin, M. C. P. van Eijk, *Angew. Chem.* **2003**, *115*, 1486–1496; *Angew. Chem. Int. Ed.* **2003**, *42*, 1448–1457; c) I. W. Hamley, *Angew. Chem.* **2003**, *115*, 1730–1752; *Angew. Chem. Int. Ed.* **2003**, *42*, 1692–1712.
- [2] J. N. Israelachvili in *Physics of Amphiphiles: Micelles Vesicles and Microemulsions* (Eds.: V. Degiorgio, M. Corti) North Holland, Amsterdam, **1985**.
- [3] a) A. Aggeli, I. A. Nyrkova, M. Bell, R. Harding, L. Carrick, T. C. B. McLeish, A. N. Semenov, N. Boden, *Proc. Natl. Acad. Sci. USA* **2001**, *98*, 11857–11862; b) B. Pokroy, S. H. Kang, L. Mahadevan, J. Aizenberg, *Science* **2009**, *323*, 237–240; c) Y. He, T. Ye, M. Su, C. Zhang, A. E. Ribbe, W. Jiang, C. Mao, *Nature* **2008**, *452*, 198–202.
- [4] a) S. Günes, H. Neugebauer, N. Serdar Sariciftci, *Chem. Rev.* **2007**, *107*, 1324–1338; b) A. A. Argun, P.-H. Aubert, B. C. Thompson, I. Schwendeman, C. L. Gaupp, J. Hwang, N. J. Pinto, D. B. Tanner, A. G. MacDiarmid, J. R. Reynolds, *Chem. Mater.* **2004**, *16*, 4401–4412; c) G. Zotti, B. Vercelli, A. Berlin, *Acc. Chem. Res.* **2008**, *41*, 1098–1109.
- [5] a) J. M. Kang, J. Rebek, *Nature* **1996**, *382*, 239–241; b) M. C. Calama, P. Timmerman, D. N. Reinhoudt, *Angew. Chem.* **2000**, *112*, 771–774; *Angew. Chem. Int. Ed.* **2000**, *39*, 755–758; c) D. Haldar, H. Jiang, J. M. Leger, I. Huc, *Angew. Chem.* **2006**, *118*, 5609–5612; *Angew. Chem. Int. Ed.* **2006**, *45*, 5483–5486; d) Y. Ferrand, A. M. Kendhale, J. Garric, B. Kauffmann, I. Huc, *Angew. Chem.* **2010**, *122*, 1822–1825; *Angew. Chem. Int. Ed.* **2010**, *49*, 1778–1781.
- [6] a) J. L. Atwood, L. R. MacGillivray, *Nature* **1997**, *389*, 469–472; b) J. M. Rivera, T. Martin, J. Rebek, *Science* **1998**, *279*, 1021–1023; c) J. Rebek, *Angew. Chem.* **2005**, *117*, 2104–2115; *Angew. Chem. Int. Ed.* **2005**, *44*, 2068–2078.
- [7] M. Ruben, J. Rojo, F. J. Romero-Salguero, L. H. Uppadine, J.-M. Lehn, *Angew. Chem.* **2004**, *116*, 3728–3747; *Angew. Chem. Int. Ed.* **2004**, *43*, 3644–3662.
- [8] a) E. D. Sone, E. R. Zubarev, S. I. Stupp, *Angew. Chem.* **2002**, *114*, 1781–1785; *Angew. Chem. Int. Ed.* **2002**, *41*, 1705–1709; b) P. G. A. Janssen, J. Vandenbergh, J. L. J. van Dongen, E. W. Meijer, A. P. H. J. Schenning, *J. Am. Chem. Soc.* **2007**, *129*, 6078–6079; c) K. Oh, K.-S. Jeong, J. S. Moore, *Nature* **2001**, *414*, 889–893; d) R. A. Smaldone, J. S. Moore, *Chem. Eur. J.* **2008**, *14*, 2650–2657.
- [9] H. Dietz, S. M. Douglas, W. M. Shih, *Science* **2009**, *325*, 725–730.
- [10] J. N. Israelachvili, H. Wennertström, *J. Phys. Chem.* **1992**, *96*, 520–531.
- [11] a) J. P. Hill, W. Jin, A. Kosaka, T. Fukushima, H. Ichihara, T. Shimomura, K. Ito, T. Hashizume, N. Ishii, T. Aida, *Science* **2004**, *304*, 1481–1483; b) W.-Y. Yang, E. Lee, M. Lee, *J. Am. Chem. Soc.* **2006**, *128*, 3484–3485; c) J.-K. Kim, E. Lee, M.-C. Kim, E. Sim, M. Lee, *J. Am. Chem. Soc.* **2009**, *131*, 17768–17770; d) V. Percec, C. H. Ahn, G. Ungar, D. J. P. Yearley, M. Moller, S. S. Sheiko, *Nature* **1998**, *391*, 161–164; e) S. D. Hudson, H.-T. Jung, V. Percec, W.-D. Cho, G. Johansson, G. Ungar, V. S. K. Balagurusamy, *Science* **1997**, *278*, 449–452.
- [12] a) R. Oda, I. Huc, M. Schmutz, S. J. Candau, F. C. MacKintosh, *Nature* **1999**, *399*, 566–569; b) A. Brizard, C. Aimé, T. Labrot, I. Huc, D. Berthier, F. Artzner, B. Desbat, R. Oda, *J. Am. Chem. Soc.* **2007**, *129*, 3754–3762; c) R. Oda, F. Artzner, M. Laguerre, I. Huc, *J. Am. Chem. Soc.* **2008**, *130*, 14705–14712.
- [13] a) A. Aggeli, M. Bell, N. Boden, J. N. Keen, P. F. Knowles, T. C. B. McLeish, M. Pitkeathly, S. E. Radford, *Nature* **1997**, *386*, 259–262; b) J. D. Hartgerink, E. Beniash, S. I. Stupp, *Science* **2001**, *294*, 1684–1688; c) H. Dong, S. E. Paramonov, J. D. Hartgerink, *J. Am. Chem. Soc.* **2008**, *130*, 13691–13695; d) S. E. Paramonov, H.-W. Jun, J. D. Hartgerink, *J. Am. Chem. Soc.* **2006**, *128*, 7291–7298.
- [14] a) M. W. Matsen, F. S. Bates, *J. Chem. Phys.* **1997**, *106*, 2436–2448; b) M. W. Matsen, F. S. Bates, *Macromolecules* **1996**, *29*, 7641–7644.
- [15] S. I. Stupp, V. LeBonheur, K. Walker, L. S. Li, K. E. Huggins, M. Keser, A. Amstutz, *Science* **1997**, *276*, 384–389.
- [16] J. N. Israelachvili, D. J. Mitchell, B. W. Ninham, *J. Chem. Soc. Faraday Trans. 2* **1976**, *72*, 1525–1568.
- [17] a) A. P. H. J. Schenning, A. F. M. Kilbinger, F. Biscarini, M. Cavallini, H. J. Cooper, P. J. Derrick, W. J. Feast, R. Lazzaroni, Ph. Leclère, L. A. McDonnell, E. W. Meijer, S. C. J. Meskers, *J. Am. Chem. Soc.* **2002**, *124*, 1269–1275; b) F. J. M. Hoebe, P. Jonkheijm, E. W. Meijer, A. P. H. J. Schenning, *Chem. Rev.* **2005**, *105*, 1491–1546.
- [18] S. Ellinger, A. Kreyes, U. Ziener, C. Hoffmann-Richter, K. Landfester, M. Möller, *Eur. J. Org. Chem.* **2007**, 5686–5702.
- [19] F. S. Schoonbeek, J. H. van Esch, B. Wegewijs, D. B. A. Rep, M. P. de Haas, T. M. Klapwijk, R. M. Kellogg, B. L. Feringa, *Angew. Chem.* **1999**, *111*, 1486–1490; *Angew. Chem. Int. Ed.* **1999**, *38*, 1393–1397.
- [20] a) C. R. G. Grenier, W. Pisula, T. J. Joncheray, K. Müllen, J. R. Reynolds, *Angew. Chem.* **2007**, *119*, 728–731; *Angew. Chem. Int. Ed.* **2007**, *46*, 714–717; b) Z. Chen, V. Stepanenko, V. Dehm, P. Prins, L. D. A. Siebbeles, J. Seibt, P. Marquetand, V. Engel, F. Würthner, *Chem. Eur. J.* **2007**, *13*, 436–449.
- [21] a) W. Jin, Y. Yamamoto, T. Fukushima, N. Ishii, J. Kim, K. Kato, M. Takata, T. Aida, *J. Am. Chem. Soc.* **2008**, *130*, 9434–9440; b) J. M. W. Chan, J. R. Tischler, S. E. Kooi, V. Bulović, T. M. Swager, *J. Am. Chem. Soc.* **2009**, *131*, 5659–5666.
- [22] a) A. Ajayaghosh, R. Varghese, V. K. Praveen, S. Mahesh, *Angew. Chem.* **2006**, *118*, 3339–3342; *Angew. Chem. Int. Ed.* **2006**, *45*, 3261–3264; b) A. Ajayaghosh, S. J. George, V. K. Praveen, *Angew. Chem.* **2003**, *115*, 346; *Angew. Chem. Int. Ed.* **2003**, *42*, 332; c) A. Ajayaghosh, V. K. Praveen, C. Vijayakumar, *Chem. Soc. Rev.* **2008**, *37*, 109–122.
- [23] a) K. Yoosaf, A. Belbakra, N. Armaroli, A. Llanes-Pallas, D. Bonifazi, *Chem. Commun.* **2009**, 2830–2832; b) V. Percec, M. Glodde, T. K. Bera, Y. Miura, I. Shiyonovskaya, K. D. Singer, V. S. K. Balagurusamy, P. A. Heiney, I. Schnell, A. Rapp, H.-W. Spiess, S. D. Hudson, H. Duan, *Nature* **2002**, *417*, 384–387.
- [24] G. Fernández, F. García, L. Sánchez, *Chem. Commun.* **2008**, 6567–6569.
- [25] a) L. Jiang, R. C. Hughes, D. Y. Sasaki, *Chem. Commun.* **2004**, 1028–1029; b) D. A. Stone, L. Hsua, S. I. Stupp, *Soft Matter* **2009**, *5*, 1990–1993.
- [26] a) C. Xia, J. Locklin, J. H. Youk, T. Fulghum, R. C. Advincula, *Langmuir* **2002**, *18*, 955–957.
- [27] J.-K. Kim, E. Lee, Y.-B. Lim, M. Lee, *Angew. Chem.* **2008**, *120*, 4740–4744; *Angew. Chem. Int. Ed.* **2008**, *47*, 4662–4666.
- [28] C. Xue, S. Velayudham, S. Johnson, R. Saha, A. Smith, W. Brewer, P. Murthy, S. T. Bagley, Haiying Liu, *Chem. Eur. J.* **2009**, *15*, 2289–2295.
- [29] K. P. R. Nilsson, P. Hammarström, *Adv. Mater.* **2008**, *20*, 2639–2645.
- [30] J. E. Reeve, H. A. Collins, K. De Mey, M. M. Kohl, K. J. Thorley, O. Paulsen, K. Clays, H. L. Anderson, *J. Am. Chem. Soc.* **2009**, *131*, 2758–2759.
- [31] M. S. Berggren, A. Richter-Dahlfors, *Adv. Mater.* **2007**, *19*, 3201–3213.
- [32] J. R. Matthews, F. Goldoni, A. P. H. J. Schenning, E. W. Meijer, *Chem. Commun.* **2005**, 5503–5505.
- [33] N. Reitzel, D. R. Greve, K. Kjaer, P. B. Howes, M. Jayaraman, S. Savoy, R. D. McCullough, J. T. McDevitt, T. Bjørnholm, *J. Am. Chem. Soc.* **2000**, *122*, 5788–5800.
- [34] M. Kasha, *Radiat. Res.* **1963**, *20*, 55–70.
- [35] W. L. Hinze, E. Pramauro, *Crit. Rev. Anal. Chem.* **1993**, *24*, 133–177.
- [36] M. C. A. Stuart, J. C. van de Pas, J. B. F. N. Engberts, *J. Phys. Org. Chem.* **2005**, *18*, 929–934.

- [37] P. van Rijn, T. J. Savenije, M. C. A. Stuart, J. H. van Esch, *Chem. Commun.* **2009**, 2163–2165; X. Cui, S. Mao, M. Liu, H. Yuan, Y. Du, *Langmuir* **2008**, *24*, 10771–10775.
- [38] L. Qiao, A. J. Easteal, *Colloid Polym. Sci.* **1998**, *276*, 313–320.
- [39] a) R. Nagarajan, *Langmuir* **2002**, *18*, 31–38; b) M. Borkovec, *Adv. Colloid Interface Sci.* **1992**, *37*, 195–217.
- [40] The shifts that were seen were in the order of 10–15 nm towards the red and this occurred gradually, suggesting inter-filter effects. For **3** a shoulder did appear at higher concentrations.
- [41] B. Valeur, *Molecular Fluorescence: Principles and Applications*, **2001**, Wiley-VCH, Weinheim.
- [42] Patrick van Rijn, Dainius Janeliunas, Aurélie M. A. Brizard, Marc C. A. Stuart, Ger J. M. Koper, Rienk Eelkema, Jan H. van Esch, *New J. Chem.* submitted.

Received: June 29, 2010  
Published online: November 16, 2010